

This is the accepted manuscript made available via CHORUS. The article has been published as:

Photonic Chern insulator through homogenization of an array of particles

Meng Xiao and Shanhui Fan

Phys. Rev. B **96**, 100202 — Published 28 September 2017

DOI: [10.1103/PhysRevB.96.100202](https://doi.org/10.1103/PhysRevB.96.100202)

Photonic Chern insulator through homogenization of an array of particles

Meng Xiao and Shanhui Fan^{*}

¹*Department of Electrical Engineering, and Ginzton Laboratory, Stanford University, Stanford, California 94305, USA*

^{*}Corresponding E-mail: shanhui@stanford.edu

Abstract: We propose a route towards creating a metamaterial that behaves as a photonic Chern insulator, through homogenization of an array of gyromagnetic cylinders. We show that such an array can exhibit non-trivial topological effects, including topologically non-trivial band gaps and one-way edge states, when it can be homogenized to an effective medium model that has the Berry curvature strongly peaked at the wavevector $k=0$. The non-trivial band topology depends only on the parameters of the cylinders and the cylinders' density, and can be realized in a wide variety of different lattices including periodic, quasi-periodic and random lattices. Our system provides a platform to explore the interplay between disorder and topology and also opens a route towards synthesis of topological meta-materials based on the self-assembly approach.

The classification of band structure in terms of band topology in classical waves has led to the newly emerging field of topological photonics and phononics. [1-32] The majority of previous works on topological photonics and phononics consider periodic structures, where the non-trivial topology arises from the scattering of waves by the periodic structure. Complementary to the developments of topological photonic and phononic crystals, however, there have also been significant recent works on topological meta-materials. [29-33] In these designs of topological metamaterials, one considered a uniform system as characterized by an electromagnetic susceptibility such as a permittivity or permeability tensor, and identified nontrivial topological features in the band structure associated with such a susceptibility.

Since the possible susceptibilities of naturally occurring materials are rather limited, for the vast majority of works on meta-materials, one considers an inhomogeneous system consisting of an array of meta-atoms, and obtains its effective susceptibility, which defines the corresponding effective medium through a homogenization procedure. Therefore, a question that is central to the development of topological metamaterial naturally arises: to what extent does the homogenization procedure preserve topological properties? This is to say, for a given effective medium that has topological features, can one construct a physical system consisting of an array of meta-atoms, which homogenizes to such an effective medium, and exhibits some of the non-trivial topological properties? This question, which is of central importance to the physical implementation of topological metamaterial, has not been addressed in previous literature on topological metamaterial and in fact is quite subtle. In spite of the existence of standard homogenization procedure, it is far from obvious, *a priori*, that the topology of a physical metamaterial system consisting of an array of sub-wavelength elements can be understood in terms of its effective medium, no matter whether such an effective medium is local or nonlocal. For an effective medium model to work, the effective wavelength, which is the length scale at which the field varies, should be much larger than the size of the unit cell. Since at the Brillouin zone boundary, the effective wavelength is always comparable with the size of the unit cell, there is no guarantee that effective medium model can be used to obtain the information about the band structure over the entire first Brillouin zone. And yet such information is necessary to determine the topology (such as the Chern number) of the band structure.

In this paper, we address the question above by constructing an effective medium in which the Berry curvature of its band structure is strongly peaked at $k = 0$, where k is the wavevector. Since the effective medium model should describe the physical structure very well near $k = 0$, we expect that the non-trivial band topology of the effective medium model should also manifest in the physical metamaterial systems. And indeed, through numerical simulations, we find that our metamaterial systems with a wide variety of lattices, including periodic, quasiperiodic, and random lattices, all of which homogenize to the same effective medium model, all possesses complete non-trivial topological band gap. We also note that only part of the topological features of the effective medium persist in the inhomogeneous physical system.

From a fundamental physics perspective, the systems that we consider here may provide a platform to explore the interplay between order or disorder and topology. From an experimental perspective, creating a disordered system with non-trivial topology may relax the stringent requirements for fabricating topologically non-trivial photonic and phononic systems. While there have been several very recent works on nontrivial topological photonic structures utilizing aperiodic lattices [34-36], our construction differs in that it is not based on any specific lattice [34,35] or needs to engineer the local connections [36]. The structure reported here may therefore open a route towards synthesis of topological meta-material based on the self-assembly approach.[37-39]

We first introduce an effective medium model that exhibits non-trivial topology in its band structure, and has the Berry curvature of its band structure strongly peaked at $k = 0$. We consider electromagnetic waves in two dimensions and focus on the TM polarization, which has the electric field E_z along the z -direction and the magnetic field H_x, H_y in the xy -plane. For such a TM polarized wave, we consider an effective medium model where the relevant effective electromagnetic materials are the relative electric permittivity ϵ_e along the z -direction, and the relative magnetic permeability in the xy -plane, which has the form $\overset{\text{T}}{\mu}_e = (\mu_r, i\mu_k; -i\mu_k, \mu_r)$. In order to achieve a band structure with non-trivial topology, we start with the case where $\mu_k = 0$, and

$$\begin{aligned}\varepsilon_e &= \gamma_\varepsilon (\omega - \omega_E) / \omega_E \\ \mu_r &= \gamma_\mu (\omega - \omega_H) / \omega_H\end{aligned}\quad (1)$$

The starting point of our system is therefore the Epsilon and Mu Near Zero (EMNZ) systems that have been widely considered in the meta-material literature. [40] Here we consider a lossless system. γ_e and γ_μ are both positive as required by causality. [41] When $\omega_E \neq \omega_H$, (Fig. (a)), the system supports a mode that is singly degenerate at $k = 0$ having a frequency $\omega = \omega_E$. This mode exhibits a quadratic dispersion at $k \neq 0$. The system also supports at $k = 0$ a pair of doubly degenerate modes at $\omega = \omega_H$. At $k \neq 0$ the two modes split into two bands, one with flat dispersion and the other with quadratic dispersion. By setting $\omega_E = \omega_H \equiv \omega_0$, we force a three-fold accidental degeneracy at $k = 0$. [42,43] At $k \neq 0$, the three modes split into two bands with a Dirac-like linear dispersion as well as a flat band, as shown in Fig. (b).

Starting with the band structure in Fig. (b), we then break time-reversal symmetry by setting a frequency-independent $\mu_k \neq 0$. Now the three-fold degeneracy at $k = 0$ is completely lifted as shown in Fig. (c) and two band gaps are introduced into the system. Both of these band gaps are topologically non-trivial. To see the nontrivial topology, here we develop a Hamiltonian for the Maxwell's equations near ω_0 . For the system with $\mu_k = 0$, an effective Hamiltonian has been developed to describe the physics in the vicinity of the triply degenerate point. [44]. For our system here with $\mu_k \neq 0$, starting from the Maxwell's equations, and keeping only the lowest order of $\Delta\omega \equiv \omega - \omega_0$ we obtain

$$\begin{pmatrix} 0 & -i\tilde{\mu}_k & \tilde{k}_y \\ i\tilde{\mu}_k & 0 & -\tilde{k}_x \\ \tilde{k}_y & -\tilde{k}_x & 0 \end{pmatrix} \begin{pmatrix} \tilde{H}_x \\ \tilde{H}_y \\ \tilde{E}_z \end{pmatrix} = \frac{\Delta\omega}{\omega_E} \begin{pmatrix} \tilde{H}_x \\ \tilde{H}_y \\ \tilde{E}_z \end{pmatrix}, \quad (2)$$

where $\tilde{\mu}_k = \mu_k / \gamma_\mu$, $\tilde{k}_{x,y}^0 = k_{x,y} c / (\omega_0 \sqrt{\gamma_\varepsilon \gamma_\mu})$, $\tilde{H}_{x,y}^0 = \sqrt{\mu_0 \gamma_\mu} H_{x,y}$, $\tilde{E}_z^0 = \sqrt{\varepsilon_0 \gamma_\varepsilon} E_z$ and c is the speed of light. Here k_x and k_y are the wavevectors, respectively. The matrix on the right-hand side of Eq. (2) can now serve as an effective Hamiltonian. The three eigenvalues of this Hamiltonian

are given by $\left\{0, \pm\sqrt{\frac{\rho_x^2}{k_x^2} + \frac{\rho_y^2}{k_y^2} + \rho_0^2}\right\}$, which is consistent with the band dispersion in Fig. (c). With the effective Hamiltonian obtained, we can determine the total Berry flux for the upper, middle, and lower bands to be $-\text{sgn}(\mu_k)2\pi$, 0 and $\text{sgn}(\mu_k)2\pi$, respectively, when $\mu_k \neq 0$. Thus we have introduced an effective medium model with topologically non-trivial band gaps. Such an effective medium model thus represents a photonic Chern insulator. While there have been many theoretical proposals and experimental demonstrations of photonic Chern insulators [4-9], the effective medium model as proposed here represents a route for creating a Chern insulator that was not previously reported. In this model, the Berry curvature peaks at $k = 0$, as shown in Fig. 1(d). Therefore, we anticipate that this effective medium model can be used to guide the construction of physical meta-material structures through homogenization.

Motivated by the effective medium model as presented above, we now consider physical metamaterial systems which homogenize to this model at $k = 0$. We first consider an individual cylinder with radius r_c , relative permittivity ϵ_c and the relative permeability in the xy -plane $\vec{\mu}_c = (1, i\kappa; -i\kappa, 1)$, where κ is assumed to be frequency independent. This is a simplified model for gyromagnetic effects. A more sophisticated model of the gyromagnetic effects can be found in Ref.[44]. The main results of the paper are not affected by the use of the more sophisticated model. The electric and magnetic dipole responses of a cylinder are described by $\vec{p} = \epsilon_0 \alpha_E \vec{E}^{\text{loc}}$ and $\vec{m}_\pm = \alpha_\pm \vec{H}^{\text{loc}}$, where \vec{E}^{loc} and \vec{H}^{loc} represent the local electric and magnetic fields, respectively, α_E and α_\pm represent respectively, the electric and magnetic dipole polarizabilities, and can be found in Supplemental Material S. I.

We then consider a metamaterial system consisting of an array of cylinders as described above. An example of such metamaterial is shown in Fig. (a). Following the procedure in Ref. [45], we derive the effective medium parameters by solving the scattering problem as illustrated in Fig. (b). Here one particle is set at the center of a cylindrical cavity filled with air and surrounded by a background consisting of the effective medium. The radius of the cylindrical cavity r_0 is chosen such that

$\pi r_0^2 / a^2 = 1$, where $1/a^2$ is the number of cylinders inside a unit area for the random array. The parameters of the effective medium are determined by assuming that there is no scattering by the cavity for waves incident from the effective medium in the limit where the wavelength in the effective medium is much larger than r_0 , in which case only the electric and magnetic dipole responses of the cylinder need to be taken into account. The no-scattering condition gives (Refer to the Supplemental Material S-I for detailed derivations.)

$$\varepsilon_e = -\frac{2 \left[4J'_0(k_0 r_0) + i\alpha_E k_0^2 H_0^{(1)'}(k_0 r_0) \right]}{k_0 r_0 \left[4J_0(k_0 r_0) + i\alpha_E k_0^2 H_0^{(1)}(k_0 r_0) \right]}, \quad (3)$$

and

$$\mu'_r m \mu'_k = \frac{k_0 r_0 \left[8J'_1(k_0 r_0) + i\alpha_\pm k_0^2 H_1^{(1)'}(k_0 r_0) \right]}{\left[8J_1(k_0 r_0) + i\alpha_\pm k_0^2 H_1^{(1)}(k_0 r_0) \right]}, \quad (4)$$

with $\mu_k = -\mu'_k / (\mu_r'^2 - \mu_k'^2)$, $\mu_r = \mu'_r / (\mu_r'^2 - \mu_k'^2)$, and k_0 is the wavevector in vacuum. $J_n(x)$, $H_n^{(1)}(x)$, $J'_n(x)$ and $H_n^{(1)'}(x)$ are the Bessel function and Hankel function of the first kind and their derivatives. It can be proved that the effective parameters as described in Eqs. (3) and (4) are purely real when the system is nonabsorptive. [45] (See also Supplemental Material S.I) When the time-reversal symmetry is preserved, i.e, when $\kappa = 0$ in $\vec{\mu}_c$, the effective parameters having the form of Eq. (1) can be achieved by choosing the parameters of the cylinders such that the electric and magnet dipole responses have the same resonant frequencies, which then results in the dispersion relation shown in Fig. (b). [42] Starting from such a cylinder, the dispersion relation in Fig. (c) can then be achieved by setting $\kappa \neq 0$ in $\vec{\mu}_c$, which breaks the time-reversal symmetry.

Using full wave simulations, we now show that different lattices of the cylinders as discussed above, all of which homogenize to the same effective medium model has described above, in fact all possesses non-trivial topology in their band structures. In Fig. (a), we consider the square lattice case. The cylinders have the parameters $r_c = 0.1735a$, $\varepsilon_c = 20$, and $\kappa = 0$, which are determined following the homogenization procedure as outlined above. The three-fold degeneracy at the Γ

point (i.e. $k = 0$ point) and conical-like dispersion near the Γ point are consistent with the effective model as plotted in Fig. (b). In fact, we can find similar band dispersions near the Γ point as those in Fig. (a)-(c) by varying some of the parameters of the cylinders. (See the Supplemental Material S. II). Based on the square lattice discussed above, we now consider the strip geometry shown in Fig. (c). The lattice consists of the same cylinder as discussed above but with $\kappa = 0.08$. The lattice is periodic along the y direction and truncated by a perfect magnetic conductor (PMC) boundary on the left and a perfect electric conductor (PEC) boundary on the right. The projected band and the corresponding surface states are shown in Fig. (b). The field distribution of one of the surface states near the PEC boundary is also shown in Fig. (c). The projected band structure consists of three groups of bulk bands. Dispersions of the upper and lower groups of bulk bands agree well with the effective medium model near the Γ point. And as predicted by the effective medium model, the breaking of time reversal symmetry introduces a local Berry flux of 2π and one-way surface states emerge near the Γ point.

On the other hand, the effective medium model does not describe the band structure for the wavevectors significantly away from the Γ point. First, the middle band is no longer perfectly flat. Second, as shown in Fig. 3a, there exists a band degeneracy between the lower two bands at the M point protected by the combination of time-reversal symmetry and the C_{4v} lattice symmetry. Such degeneracy is not predicted by our effective medium model. When this degeneracy is lifted by breaking the time-reversal symmetry, a Berry flux of 2π peaks at the M point and as a result, the lower band becomes topologically trivial. The surface states inside the lower band gap, emerge near the Γ point, almost reach the other band, but then merge back into their original bands.

In the square lattice structure, we observe that the effective medium model of Fig. generally agrees well with the band structure of the physical system near Γ point. Moreover, the upper band of Fig. in the effective medium model agrees quite well with the band structure of the physical system. As a result one can achieve a topologically non-trivial band gap between the upper and the middle band in the physical systems. And a one-way edge state can be found in such a band gap in a truncated lattice. The lower band, on the other, significantly differs from the effective medium model away from Γ .

These observations turn out to be generally applicable for other lattices that homogenize to the same effective medium model. As an additional example, results for a triangular lattice are shown in Supplemental Materials S. III. Therefore, we have shown that the effective medium model as we developed here provides the guidance for creating a class of non-trivial topological meta-material with different periodic lattices.

We now show that the effective medium model can be used to guide us in constructing random or quasi-periodic system with a non-trivial topological band gap and a one-way edge state. The evolution of the band structures from a square lattice to a completely random lattice is discussed in Supplemental Material Sec. VI. As an exemplary demonstration of random systems, we consider a geometry with a supercell as shown in Fig. (a). The supercell forms a square lattice and each supercell contains 25 cylinders with the same radius, dielectric constant and density of cylinders as in Fig. (b), except with $\kappa = 0.4$. Within each supercell, the cylinders are randomly distributed with equal probability while keeping the minimal distances between cylinders to be larger than $0.8a$ so that the dipole approximation remains valid. The projected band structure for a strip geometry with 5 supercells along the y direction is shown in Fig. 4a. The strip is truncated in the y -direction with PEC boundaries on the upper and lower sides, and is assumed to be periodic along the x direction. The structure supports a topological non-trivial band gap, the frequency range of which corresponds to the upper band gap in the effective medium model. Within the gap the structure supports one-way surfaces states with opposite propagation direction on the upper and lower boundaries, respectively (blue and red curves in Fig. (a)). These features are consistent with the effective medium model. We also note that in the effective medium model the upper edge of this nontrivial band gap corresponds to $\mu_{\text{eff}} = 0$, while the lower edge corresponds to $\mu_{\text{eff}} \rightarrow \infty$. (See Supplemental Material Sec. I) This feature is consistent with Ref. [46]. However, the interaction in Ref. [46] is short-ranged (only limited to particles within a finite distance), our construction does not make assumptions about the ranges of interactions between particles, and the electromagnetic interaction between particles in the array systems similar to ours is typically not short-ranged.

The existence of one-way edge state in a random system can also be visualized by simulating a finite

system as shown in Fig. (b). The cylinders are the same as Fig. (a) and the minimal distances between cylinders are also kept to be larger than $0.8a$. This lower-side of the finite system is truncated by a perfectly matched layer [47] to absorb the wave. The remaining boundaries of the system consist of PEC. The wave propagates anticlockwise without being backscattered when the frequency of the source is inside the nontrivial bandgap. While here we show an example of a random lattice, similar effects of band gap and one-way edge states are also observed in other isotropic systems such as quasicrystals with the same cylinder and cylinder density. (See Supplemental Material Sec. IV)

In conclusion, we theoretically propose and numerically demonstrate a route towards creating a metamaterial that behaves as a photonic Chern insulator, through homogenization of an array of particles. While for concreteness we have considered cylindrical particle possessing gyromagnetic effects, one can achieve similar results with gyroelectric effects more commonly used in the optical frequency range. Also the particles can be of other shapes provided that their response can be well described by the electric and magnetic polarizabilities. Our method can easily be extended to create meta-materials that achieve electromagnetic analogues of quantum spin Hall systems, and be generalized for other classical wave systems.

This work is supported by the U. S. Air Force of Scientific Research (Grant No. FA9550-12-1-0471), and the U. S. National Science Foundation (Grant No. CBET-1641069). M. X. thanks Dr. S. B. Wang for help with COMSOL simulations.

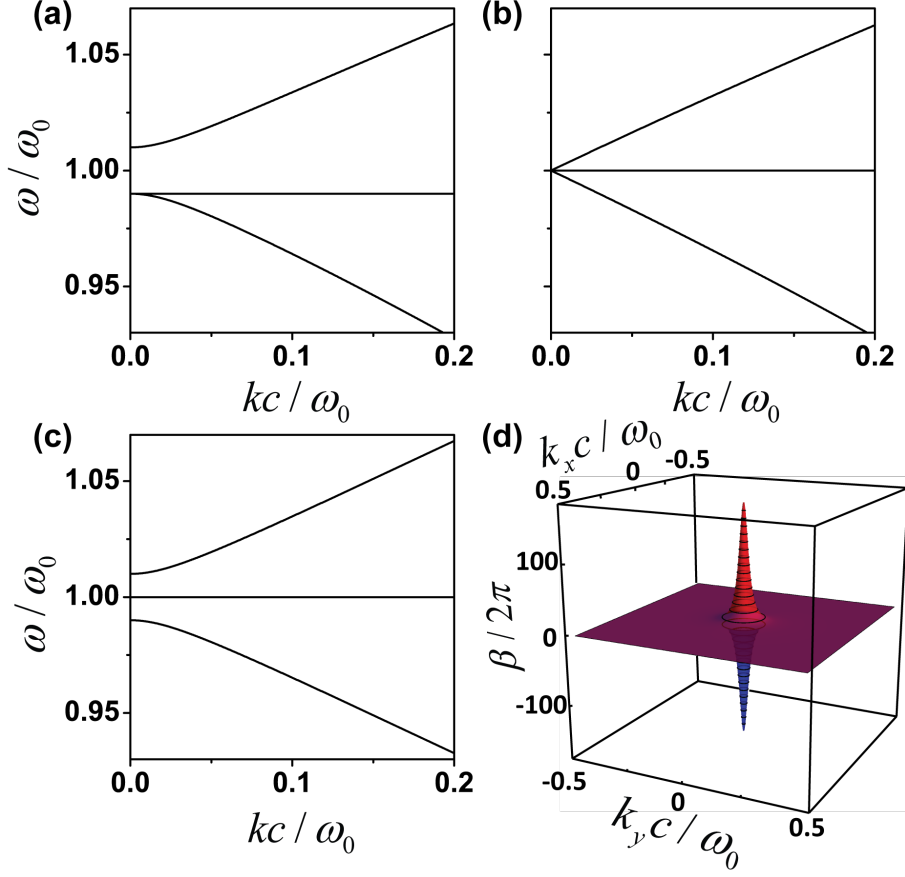


Fig. 1 (color online). The dispersion relation for the system as described by Eq. (1) with $\gamma_\epsilon = \gamma_\mu = 3$. ω_0 is a reference frequency, c is the speed of light in vacuum and k is the in-plane wave vector. (a) $\omega_E = 1.01\omega_0$, $\omega_H = 0.99\omega_0$, $\mu_k = 0$. (b) $\omega_E = \omega_H = \omega_0$ and $\mu_k = 0$. (c) $\omega_E = \omega_H = \omega_0$ and $\mu_k = 0.03$. (d) Red and blue represent the Berry flux β of the highest and lowest bands in (c), respectively. The Berry flux of the middle band in (c) is exactly zero.

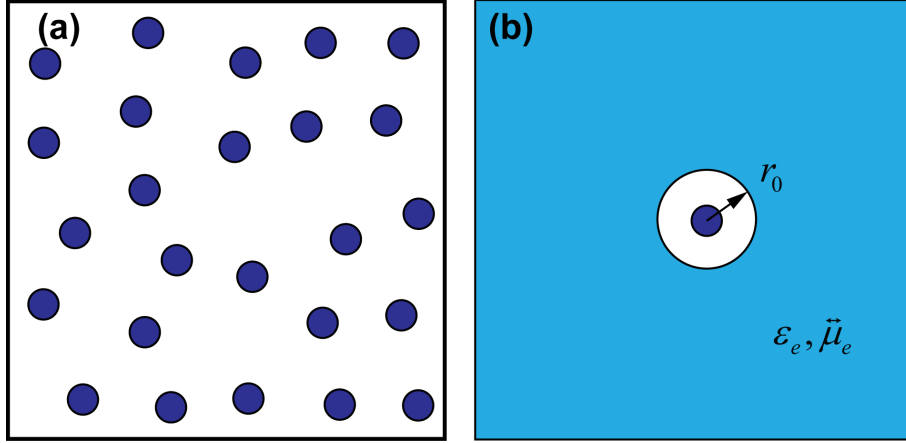


Fig. 2(color online). (a) A system consisting of a random array of cylindrical particles (solid blue disks). Each particle is described by its electric and magnetic dipole responses to external electromagnetic fields. There are in total 25 cylinders with the same radius in (a). The cylinders are randomly distributed with equal probability while keeping the minimal distances between cylinders to be larger than $0.8a$, where $1/a^2$ represents the density of cylinder. (b) A sketch showing the geometry used in deriving the effective parameters, ϵ_e and $\vec{\mu}_e$, which provide an effective medium model for the array in (a). The light blue regions is filled uniformly with material having such effective parameters.

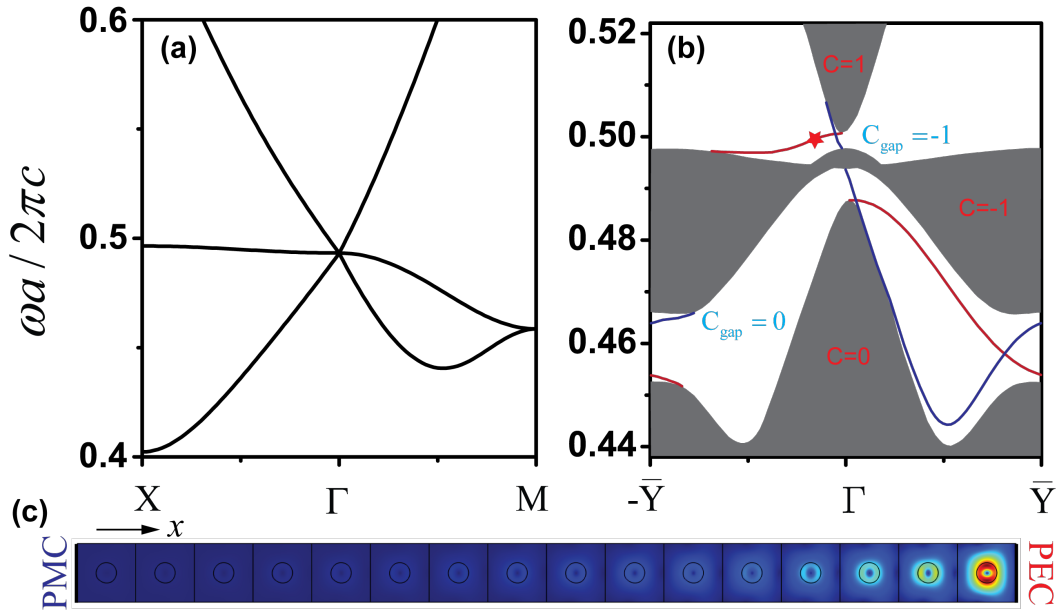


Fig. 3 (color online). (a) The band structure of cylinders in a square lattice. (b) Projected band structure (gray area) and corresponding surface states with the supercell in (c). This supercell is

terminated by a PMC boundary on the left and PEC boundary on the right. Here red and blue curves represent the surface states at the PEC and PMC boundaries, respectively. The Chern numbers for the band and the gap Chern numbers in (b) are labeled in red and cyan, respectively. The electric field amplitude of the surface state marked by red star ($k_y a / \pi = -0.2$) in (b) is also shown in (c), where red and blue colors represent maximum and zero field amplitudes, respectively. The cylinder has a radius of $r_c = 0.1735a$, where a represents the lattice constant of the square lattice. The relative permittivity of the cylinders is $\epsilon_c = 20$. $\kappa = 0$ in (a) and $\kappa = 0.08$ in (b) and (c).

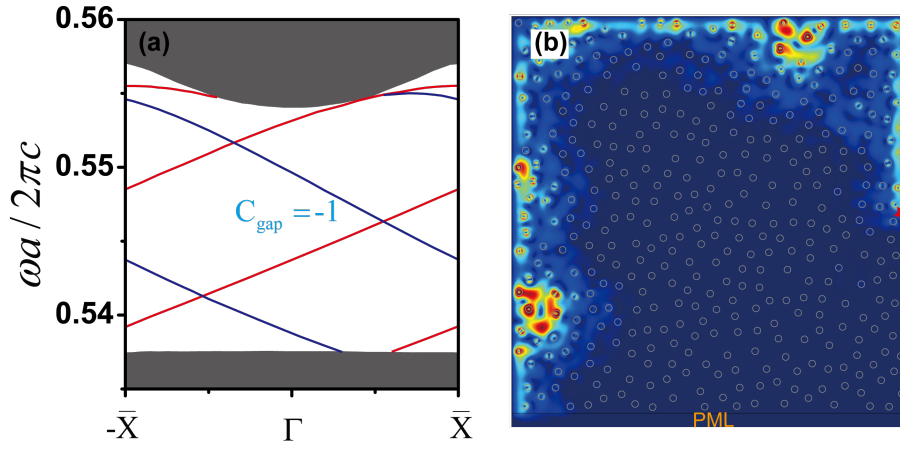


Fig. 4 (color online). (a) The projected bulk band structure (gray regions) and the band structure of surface states (red and blue curves) of a strip geometry consists of 5 of the supercells, each of which is shown in Fig. (a). The upper and lower boundaries of the strip are terminated by PECs and the strip is periodic along the horizontal direction. The blue and red curves represent the surface states on the upper boundary and the lower boundary, respectively. (b) One-way edge modes supported by a finite random lattice of cylinders. Here the red star marks the position of the source with an operating frequency at $\omega a / (2\pi c) = 0.547$. The rectangles on the lower end of the figure represents a perfectly matched layer (PML) region that absorbs the waves. All the other outer boundaries in (b) are PEC. The radius of the cylinder and the relative permittivity are $r_c = 0.1735a$ and 20, respectively, where $1/a^2$ is the density of the cylinders, and $\kappa = 0.4$.

- [1] L. Lu, J. D. Joannopoulos, and M. Soljačić, *Nat. Photonics* **8**, 821 (2014).
- [2] L. Lu, J. D. Joannopoulos, and M. Soljačić, *Nat. Phys.* **12**, 626 (2016).
- [3] S. D. Huber, *Nat. Phys.* **12**, 621 (2016).
- [4] F. D. M. Haldane and S. Raghu, *Phys. Rev. Lett.* **100**, 013904 (2008).
- [5] Z. Wang, Y. D. Chong, J. D. Joannopoulos, and M. Soljačić, *Nature (London)* **461**, 772 (2009).
- [6] Z. Wang, Y. D. Chong, J. D. Joannopoulos, and M. Soljačić, *Phys. Rev. Lett.* **100**, 013905 (2008).
- [7] K. Fang, Z. Yu, and S. Fan, *Nat. Photonics* **6**, 782 (2012).
- [8] Z. Yu, G. Veronis, Z. Wang, and S. Fan, *Phys. Rev. Lett.* **100**, 023902 (2008).
- [9] L. Yuan, Y. Shi, and S. Fan, *Opt. Lett.* **41**, 741 (2016).
- [10] M. C. Rechtsman, J. M. Zeuner, Y. Plotnik, Y. Lumer, D. Podolsky, F. Dreisow, S. Nolte, M. Segev, and A. Szameit, *Nature (London)* **496**, 196 (2013).
- [11] M. Hafezi, E. A. Demler, M. D. Lukin, and J. M. Taylor, *Nat. Phys.* **7**, 907 (2011).
- [12] M. Hafezi, S. Mittal, J. Fan, A. Migdall, and J. M. Taylor, *Nat. Photonics* **7**, 1001 (2013).
- [13] A. B. Khanikaev, S. Hossein Mousavi, W.-K. Tse, M. Kargarian, A. H. MacDonald, and G. Shvets, *Nat. Mater.* **12**, 233 (2013).
- [14] W.-J. Chen, S.-J. Jiang, X.-D. Chen, B. Zhu, L. Zhou, J.-W. Dong, and C. T. Chan, *Nat. Commun.* **5** (2014).
- [15] G. Q. Liang and Y. D. Chong, *Phys. Rev. Lett.* **110**, 203904 (2013).
- [16] E. Prodan and C. Prodan, *Phys. Rev. Lett.* **103**, 248101 (2009).
- [17] M. Xiao, G. Ma, Z. Yang, P. Sheng, Z. Q. Zhang, and C. T. Chan, *Nat. Phys.* **11**, 240 (2015).
- [18] Z. Yang, F. Gao, X. Shi, X. Lin, Z. Gao, Y. Chong, and B. Zhang, *Phys. Rev. Lett.* **114**, 114301 (2015).
- [19] C. L. Kane and T. C. Lubensky, *Nat. Phys.* **10**, 39 (2014).
- [20] L.-H. Wu and X. Hu, *Phys. Rev. Lett.* **114**, 223901 (2015).
- [21] R. Süssstrunk and S. D. Huber, *Science* **349**, 47 (2015).
- [22] X. Cheng, C. Jouvaud, X. Ni, S. H. Mousavi, A. Z. Genack, and A. B. Khanikaev, *Nat. Mater.* **15**, 542 (2016).
- [23] F. Gao *et al.*, *Nat. Commun.* **7**, 11619 (2016).
- [24] L. Lu, C. Fang, L. Fu, S. G. Johnson, J. D. Joannopoulos, and M. Soljačić, *Nat. Phys.* **12**, 337 (2016).
- [25] A. Slobozhanyuk, S. H. Mousavi, X. Ni, D. Smirnova, Y. S. Kivshar, and A. B. Khanikaev, *Nat. Photonics* **11**, 130 (2017).
- [26] L. Lu, L. Fu, J. D. Joannopoulos, and M. Soljačić, *Nat. Photonics* **7**, 294 (2013).
- [27] M. S. Rudner, N. H. Lindner, E. Berg, and M. Levin, *Phys. Rev. X* **3**, 031005 (2013).
- [28] M. Xiao, W.-J. Chen, W.-Y. He, and C. T. Chan, *Nat. Phys.* **11**, 920 (2015).
- [29] M. G. Silveirinha, *Phys. Rev. B* **92**, 125153 (2015).
- [30] W. Gao, M. Lawrence, B. Yang, F. Liu, F. Fang, B. Béri, J. Li, and S. Zhang, *Phys. Rev. Lett.* **114**, 037402 (2015).
- [31] F. Liu and J. Li, *Phys. Rev. Lett.* **114**, 103902 (2015).
- [32] M. Xiao, Q. Lin, and S. Fan, *Phys. Rev. Lett.* **117**, 057401 (2016).
- [33] S. A. H. Gangaraj, M. G. Silveirinha, and G. W. Hanson, *IEEE J. Multiscale and Multiphys. Comput. Techn.* **2**, 3 (2017).
- [34] M. A. Bandres, M. C. Rechtsman, and M. Segev, *Phys. Rev. X* **6**, 011016 (2016).
- [35] P. Titum, N. H. Lindner, M. C. Rechtsman, and G. Refael, *Phys. Rev. Lett.* **114**, 056801 (2015).
- [36] A. Agarwala, and V. B. Shenoy, *arXiv: 1701.00374v1*.
- [37] K. A. Arpin *et al.*, *Nat. Commun.* **4**, 2630 (2013).
- [38] S.-H. Kim, S. Y. Lee, S.-M. Yang, and G.-R. Yi, *NPG Asia Mater* **3**, 25 (2011).
- [39] Y. Xia, B. Gates, and Z. Y. Li, *Adv. Mater.* **13**, 409 (2001).
- [40] J. Zhang, Z. Sun, and B. Yang, *Curr. Opin. Colloid Interface Sci.* **14**, 103 (2009).

- [41] G. W. Milton, D. J. Eyre, and J. V. Mantese, Phys. Rev. Lett. **79**, 3062 (1997).
- [42] X. Huang, Y. Lai, Z. H. Hang, H. Zheng, and C. T. Chan, Nat. Mater. **10**, 582 (2011).
- [43] F. Liu, Y. Lai, X. Huang, and C. T. Chan, Phys. Rev. B **84**, 224113 (2011).
- [44] D. M. Pozar, *Microwave Engineering* (Wiley, 2012).
- [45] Y. Wu, J. Li, Z.-Q. Zhang, and C. T. Chan, Phys. Rev. B **74**, 085111 (2006).
- [46] N. P. Mitchell, L. M. Nash, D. Hexner, A. Turner, and W. T. M. Irvine, arXiv: 1612.09267v1.
- [47] J.-P. Berenger, J. Comput. Phys. **114**, 185 (1994).